Synthetic random flux model in a periodically driven optical lattice

Jan Major,[1] Marcin Płodzień,[1,2] Omjyoti Dutta,[3] and Jakub Zakrzewski[1,4]
[1]*Instytut Fizyki imienia Mariana Smoluchowskiego, Uniwersytet Jagielloński, Łojasiewicza 11, 30-348 Kraków, Poland*
[2]*Eindhoven University of Technology, P.O. Box 513, 5600 MB Eindhoven, The Netherlands*
[3]*Donostia International Physics Center (DIPC), Manuel de Lardizbal 4, E-20018 San Sebastian, Spain*
[4]*Mark Kac Complex Systems Research Center, Jagiellonian University, Łojasiewicza 11, 30-348 Kraków, Poland*
(Received 29 June 2017; published 15 September 2017)

We propose a realization of a synthetic random flux model in a two-dimensional optical lattice. Starting from Bose-Hubbard Hamiltonian for two atom species, we show how to use fast-periodic modulation of the system parameters to construct a random gauge field. We investigate the transport properties of such a system and describe the impact of time-reversal symmetry breaking and correlations in disorder on Anderson localization length.

DOI: 10.1103/PhysRevA.96.033620

I. INTRODUCTION

The fractional quantum Hall effect (QHE) has been effectively described by the Chern-Simons field theory [1,2] in which quasiparticles are weakly interacting fermions constructed by attaching an even number of flux quanta to the electrons under a Chern-Simons transformation [3]. In such a case, fractional QHE is effectively mapped into integer QHE for the composite fermions suspended in an effective magnetic field. At filling factor $\nu_f = 1/2$, the effective magnetic field vanishes and composite fermions are subject to random fluctuations of the gauge field induced by the ordinary impurities. In this context, it is important to study the localization properties of noninteracting charged particles in the presence of a random magnetic field to understand the half-filling system. The problem of charged particles moving in a random magnetic field is also relevant to theoretical studies of high-T_c models where gauge field fluctuations could significantly alter the critical temperature in high-T_c superconductors [4].

Anderson (strong) localization (AL) follows its precursor, a "weak localization" which describes a reduction of the conductivity due to constructive interferences between electronic paths and their time-reversed counterparts that hold at finite temperatures and a regime of small disorder. Because of the electron-electron and electron-phonon interactions, a direct observation of Anderson localization in solid-state systems is an impossible task and one has to rely on conductance measurements (for review, see Ref. [5]). Still it has been directly observed in experiments with light [6–9], microwaves [10], ultrasound [11], and ultracold quantum gases experiments [12–17]. Scaling theory of localization predicts that in two-dimensional (2D) noninteracting particles are Anderson localized, as an effect of quantum interference between time-reversal symmetric paths. Standard disordered systems with time-reversal symmetry have coherent backward scattering, which results in the weak localization. The symmetry class of the problem could be changed (thus qualitatively changing results), for example, by addition of the spin-orbit coupling, which creates antilocalization correction, leading to an appearance of the mobility edge in two-dimensional systems [18,19]. Another possible route is an addition of the magnetic field which breaks the time-reversal symmetry, destroys the interference effects, and results in the suppression of the weak-localization correction [20–22], leading to an increase of the localization length. The case of random flux model (RFM), where disorder appears as a random gauge field, is a subclass of systems with broken time-reversal symmetry. The existence of the mobility edge for RFM in two dimensions was for a long time a controversial issue with different predictions: Some of them conclude that there exist extended states [23–28] while other conclude that the localization length in the vicinity of the band center is just extremely big so it could not be determined numerically [29–31]. The RFM model with the diagonal disorder presents the interesting interplay between the two effects: Upon the appearance of random fluxes, Anderson localization is weakened by breaking of the time-reversal symmetry and simultaneously strengthened by the appearance of a flux disorder [32,33].

Cold atoms provide a particularly good environment for investigating AL. The ultracold atomic gases, especially "artificial crystals" (the optical lattices), provide an unprecedented tunability of almost all parameters. The factors important for the localization such as the dimensionality of the system or the disorder distribution could be controlled. The interactions could be switched off with the help of the Feshbach resonances [36]. The off-diagonal disorder and particularly random complex tunnelings—equivalent to random fluxes of gauge field—could be created by the means of the fast periodic modulation [34,35].

In this paper, we propose an experimental scheme allowing the construction of the two-dimensional lattice system with synthetic random magnetic fields. We show that time-reversal symmetry breaking does not always lead to an increase of localization length. We investigate transport properties of systems, propose and analyze a competition between the strengthening and the weakening of the localization by an introduction of random fluxes, and present a simple toy model explaining an unexpectedly strong localization in some of cases with correlations.

The article is structured as follows: In Sec. II we describe the model we use, a two-dimensional Bose-Hubbard Hamiltonian for two atomic species. The first species, forming a diagonal disorder, is composed of immobilized atoms randomly distributed in the lattice. A second one is formed by mobile atoms that interact only with immobile atoms. Artificial gauge

field is created by simultaneous fast periodic modulation of the mobile-immobile atoms interactions and a lattice height. Further in Sec. III, we present results of the numerical calculation of the localization length. We identify observed phenomena and present a simple model of transport through one plaquette to justify appearing discrepancies of localization length from the expected behavior. Finally, in Sec. IV we conclude.

II. THE MODEL

In order to create a disordered potential in the optical lattice, we consider randomly distributed *frozen* particles (f superscript) with repulsive interactions. A second species of atoms (*mobile*) are noninteracting bosons experiencing *frozen* atoms as a disorder potential. For a deep lattice, the system may be described by Bose-Hubbard model:

$$H_0 = \sum_d \sum_{\langle ij\rangle_d} \left(t a_i^\dagger a_j + t^{\mathrm{f}} a_i^{\mathrm{f}\dagger} a_j^{\mathrm{f}}\right) + \sum_i \frac{U}{2} n_i(n_i-1) + \frac{U^{\mathrm{f}}}{2} n_i^{\mathrm{f}}\left(n_i^{\mathrm{f}}-1\right) + V n_i^{\mathrm{f}} n_i, \quad (1)$$

where i is the lattice site, a_i and $a_i^\dagger$ are bosonic annihilation and creation operators respectively, n_i is a particle number operator, t is a hopping amplitude between nearest neighbors, U and V are intraspecies and interspecies contact interaction strengths, respectively, and $\langle ij\rangle_d$ denotes summing over the nearest neighbors in a direction d which could be either x or y. To obtain an appropriate disordered potential, we envision the following scenario: At the beginning, only the frozen particles are present in the lattice. By setting $t^{\mathrm{f}} \gtrsim U^{\mathrm{f}}$, we put the system into a deep superfluid state. Now, the tunnelings are changed rapidly, for example, by a fast increase of the lattice depth, and the occupation of the lattice sites after the quench will be random and given by the Poisson distribution with the mean ρ^{f} (mean occupation of the frozen particles). Into such a prepared system, the mobile particles could be injected. As we assume that $t^{\mathrm{f}} = 0$ and additionally that the mobile particles interact only with the frozen ones ($V \neq 0$ and $U = 0$, where the latter is obtained by the means of an optical or microwave Feshbach resonance [36]), we get the Hamiltonian

$$H_{\mathrm{d}} = t \sum_d \sum_{\langle ij\rangle_d} a_i^\dagger a_j + \left(V n_i^{\mathrm{f}}\right) n_i. \quad (2)$$

As a distribution of the frozen particles is now fixed, we could treat n_i^{f} as a number and consequently the last term of the Hamiltonian (2) as just the on-site energy ($\epsilon_i = V n_i^{\mathrm{f}}$). This means that the Hamiltonian (2) describes a two-dimensional system with the diagonal (onsite) disorder taken from the discrete Poisson distribution. In the next step, we want to add a gauge field to this picture. As having the gauge field in the lattice is equivalent to adding complex phases to the tunnelings, we will proceed with creating complex phases using a fast periodic modulation of the lattice parameters. In our case, we use the simultaneous modulation of the interspecies interaction $V \to V_0 + V_1 \sin(\omega t)$ and the tunneling rates $t \to t_0 + t_1^{(\mathrm{d})} f_\omega(t)$, where ω is the frequency of modulation and $f_\omega(t)$ is some periodic function. An important point is that we allow different modulations of the tunneling rates in different lattice directions. In an experiment, the modulation of the interactions could be obtained by changing a magnetic field in the vicinity of the Feshbach resonance [37,38], while the tunneling rates could be changed by the modulation of the lattice depth. The time-dependent Hamiltonian reads

$$H(t) = \sum_d \left[t_0 + t_1^{(\mathrm{d})} f_\omega(t)\right] \sum_{\langle ij\rangle_d} a_i^\dagger a_j + \sum_i \left[(V_0 + V_1 \sin\omega t) n_i^{\mathrm{f}}\right] n_i. \quad (3)$$

$H(t)$ is time periodic, so we use Floquet theory [39–41] to decouple fast micromotion from long-term dynamics described by a time-independent effective Hamiltonian. Obtaining the exact effective Hamiltonian is usually a formidable task, but the approximate result could be calculated using the Magnus expansion [40,42], providing a series in powers of $1/\omega$. In most of the cases, the convergence rate of the series could be enhanced by a transformation to a rotating frame; alas, in our case it is impossible as time-dependent terms do not commute with each other. Nevertheless, we could make a partial transformation,

$$\mathcal{U} = \exp\left(i V_1 \cos\omega t/\omega \sum_i n_i^{\mathrm{f}} n_i\right), \quad (4)$$

which removes the time dependence from the onsite part of the Hamiltonian and more importantly takes the system to a frame in which the modulation is a symmetric function of time (which makes the odd elements of the Magnus expansion identically 0 [43]):

$$H'(t) = \mathcal{U} H(t) \mathcal{U}^\dagger = \sum_i \left(V_0 n_i^{\mathrm{f}}\right) n_i + \sum_d \left[t_0 + t_1^{(\mathrm{d})} f_\omega(t)\right] \sum_{\langle ij\rangle_d} e^{i\frac{V_1}{\omega}\left(n_j^{\mathrm{f}} - n_i^{\mathrm{f}}\right)\cos\omega t} a_i^\dagger a_j. \quad (5)$$

In this frame, the 0th order of the Magnus expansion (simply a time average of the Hamiltonian) already gives the result with an error of the order of $1/\omega^2$[44]:

$$H_{\mathrm{eff}} = \langle H'(t)\rangle_T = \sum_d \sum_{\langle ij\rangle_d} J_{ij}^d[f_\omega] a_i^\dagger a_j + \left(V_0 n_i^{\mathrm{f}}\right) n_i, \quad (6)$$

where $\langle . \rangle_T$ stands for a time averaging over period $T = 2\pi/\omega$. The exact form of the effective tunneling rate J_{ij}^d depends on the procedure of modulation f_ω. We consider two different cases. First is the harmonic modulation:

$$J_{ij}^d[\cos\omega t] = \left\langle \left(t_0 + t_1^{(\mathrm{d})} \cos\omega t\right) e^{i\frac{V_1}{\omega}\left(n_j^{\mathrm{f}} - n_i^{\mathrm{f}}\right)\cos\omega t}\right\rangle_T = t_0 \mathcal{J}_0\left[\frac{V_1}{\omega}\left(n_j^{\mathrm{f}} - n_i^{\mathrm{f}}\right)\right] + i t_1^{(d)} \mathcal{J}_1\left[\frac{V_1}{\omega}\left(n_j^{\mathrm{f}} - n_i^{\mathrm{f}}\right)\right], \quad (7)$$

where $\mathcal{J}_n(x)$ is nth-order Bessel function. If we set $t_1^{(d)} = \pm\sqrt{2} t_0$, Eq. (7) could be approximated as

$$J_{ij}^d[\cos\omega t] \approx \tilde{J}_{ij}^d[\cos\omega t] = t_0 \exp\left(\pm i \tan^{-1}\left[\frac{V_1}{\omega}\left(n_j^{\mathrm{f}} - n_i^{\mathrm{f}}\right)\right]\right). \quad (8)$$

Although that approximation works only in the close vicinity of zero, especially for the phase, we will use it in calculations alongside the exact form (7). $\tilde{J}^d_{ij}[\cos\omega t]$ has several favorable features: Its amplitude is always one, so only random fluxes are present (no random tunneling amplitudes); its phase depends nonlinearly on the argument, so in the case of the symmetric modulation in both directions ($t_1^{(x)} = t_1^{(y)}$) we could expect nonvanishing fluxes; and $\tan^{-1}$ saturates on $\pm\pi/2$ and consequently the fluxes takes values smaller than 2π (2π is reached asymptotically for a very strong modulation) so the flux amplitude is monotonic function of the modulation strength.

A second option are periodic δ kicks $\text{Ш}_\omega(t) = \sum_n \delta(t + \frac{2\pi}{\omega}n)$, which gives

$$J^d_{ij}[\text{Ш}_\omega] = t_0 \exp\left[\pm\frac{V_1}{\omega}\left(n^{\rm f}_j - n^{\rm f}_i\right)\right]. \tag{9}$$

It has the desired property of the constant amplitude, but unluckily its phase is changing linearly, so only for $t_1^{(x)} \neq t_1^{(y)}$ we will get nontrivial fluxes. Furthermore, its phase will wind up, and as a result it is possible to get smaller fluxes for stronger modulation and/or larger variation of particle number. Although this modulation procedure could seem to be experimentally demanding, it could be easily approximated by the sum of the harmonic modulations: $t_1^{(\rm d)}(\cos\omega t + \cos 2\omega t + \cos 3\omega t + \cdots)$, for $t_1^{(\rm d)} = \pm 2t_0$. In contrast to the previous case, here we have a very fast convergence both for the amplitude and the phase.

In our model, the diagonal disorder is obviously correlated with the off-diagonal one, as both are taken from the same distribution of the frozen particles. It is worth checking what impact on the localization this correlation has. To that end, we consider also a different model in which we pick the onsite energies and tunnelings independently. Such a model with uncorrelated disorders is also possible to be experimentally realized; it could be created, for example, by using two different types of frozen atoms. Yet another variation we consider is a model with solely diagonal disorder placed in a staggered gauge field. A reason for introducing that model is to distinguish effects due to breaking of the time-reversal symmetry from those created by an appearance of a new type of disorder.

III. RESULTS

In order to calculate the Anderson localization length for system with diagonal and off-diagonal disorder we use the modified MacKinnon and Kramer method [34,45]. We numerically calculate two-point Green's function in a quasi-one-dimensional stripe of size $M \times N$, where we increase N to obtain a desired convergence. Each ith slice of a stripe is described by a one-dimensional Hamiltonian H_i which is coupled to $(i+1)$-th slice by $H_{i+1,j}$ matrix element. Exponential decay of Green's function smallest eigenvalue allows us to extract the localization length, $\lambda_M(E)$, as a function of energy for a fixed disorder amplitude. Next, by changing stripe width M from 16 to 128 lattice sites we analyze the scaling behavior of $\lambda_M(E)/M$ and extract two-dimensional Anderson localization length [46].

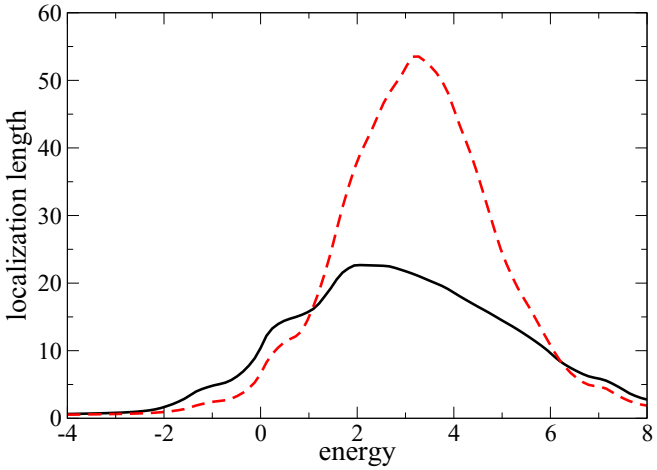

FIG. 1. Anderson localization length (in units of the lattice constant) in function of the energy (in units of tunneling amplitude). Diagonal disorder is given by Poisson distribution of frozen atoms (with mean $\rho_{\rm f} = 2.5$) and interaction amplitude $V_0 = 1.5$. Black solid curve is for undriven system and red dashed is for δ modulation (9) with modulation parameter $V_1/\omega = 1$ (for the correlated disorder case).

In calculations, we have used all three forms of effective tunneling described in the preceding section. For harmonic modulation of lattice height $J^d_{ij}[\cos(\omega t)]$ (7) and its approximation $\tilde{J}^d_{ij}[\cos(\omega t)]$ (8) we consider cases of symmetric $t_1^{(\rm x)} = t_1^{(\rm y)}$ as well as antisymmetric $t_1^{(\rm x)} = -t_1^{(\rm y)}$ modulation. For the δ modulation $J^d_{ij}[\text{Ш}_\omega]$ (9) only the antisymmetric case is calculated as the symmetric one gives no flux trivially. All presented results are calculated for interpecies interactions value $V_0 = 1.5$ (which effectively marks the scale of the onsite disorder). Qualitatively results for different V_0 values are similar but for smaller V_0 numerical errors grow due to a rapidly growing localization length, while for the stronger disorder the features become less distinctive. The mean density of frozen particles is fixed to $\rho_{\rm f} = 2.5$. Because of the discrete character of the disorder used, there is a risk that for some energies and specific occupations of frozen particles the resonant transport will occur and significantly alter the results. To check if it is an issue in our case, we have done calculations for disorder taken from the folded normal distribution (with mean $\rho_{\rm f}$ and variance $\sqrt{\rho_{\rm f}}$), which greatly resembles the Poisson distribution. Results obtained in this way do not differ significantly.

Figure 1 presents the localization length as a function of energy for two cases: without the modulation and for a strong δ modulation. The behavior shown is typical for considered systems. We do not observe the mobility edge or separated extended states so we could rely on the maximal localization length (MLL)—a maximal value of the localization length in the interval of energies studied—as a good measure of the overall transport properties of the system for given parameters.

In Fig. 2, the MLL is plotted as a function of the modulation amplitude V_1/ω. The upper panel shows results for the antisymmetric harmonic modulation [comparing the exact (7) and the approximate (8) variants], in the lower panel results for δ modulation (9) are presented. In both cases, models

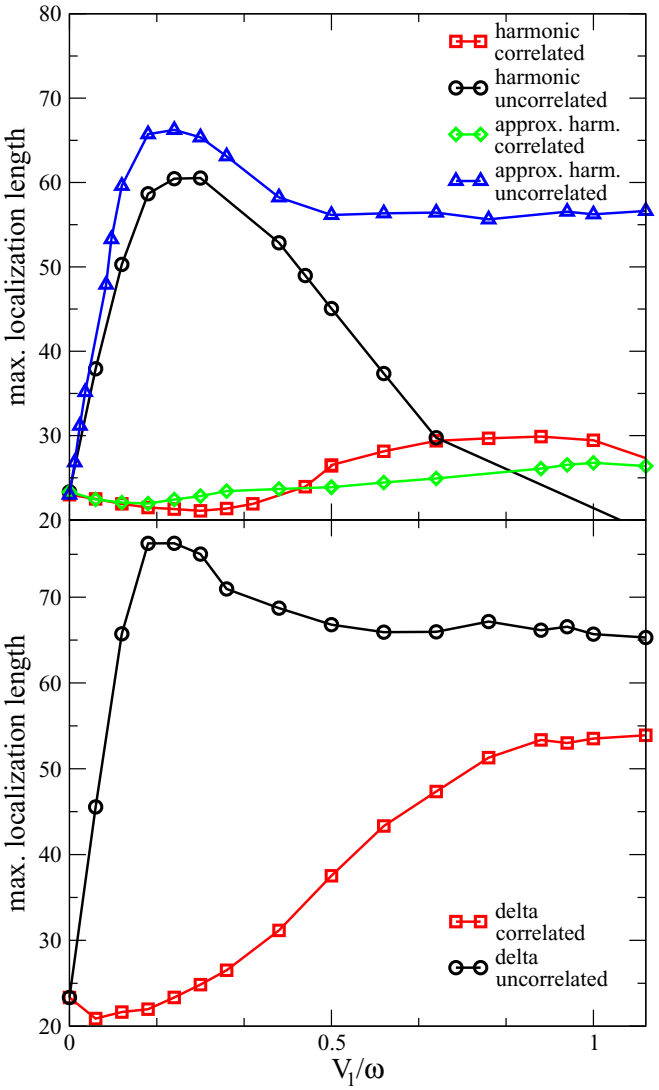

FIG. 2. The maximum localization length (in units of the lattice constant) as a function of the parameter of modulation V_1/ω. Top: Antisymmetric lattice modulation $t_1^{(x)} = -t_1^{(y)}$. Red squares and black disks shows results for harmonic modulation (7) for correlated and uncorrelated disorder respectively. Green diamonds and blue triangles are results for approximated harmonic modulation (8) also for correlated and uncorrelated cases. Bottom: Results for δ lattice modulation (9) red squares are results for diagonal disorder correlated with off-diagonal, while black circles are for uncorrelated case (lines are guides for the eye).

with correlated and uncorrelated disorder are considered. Regardless, the correlations between diagonal and off-diagonal disorder, the approximate results for the harmonic modulation (8) agree well with the exact results (7) for V_1/ω up to 0.4; see upper panel of Fig. 2. For modulations $V_1/\omega \gtrsim 0.4$, the amplitude of expression (7) starts to significantly differ from 1, and the disorder that appears in absolute values of the tunneling amplitudes seems to lower significantly the localization length.

The most striking of the observed effects is the large discrepancy between the results for the correlated and uncorrelated disorder, visible for all three considered effective tunnelings (both panels of Fig. 2). In the uncorrelated case, the

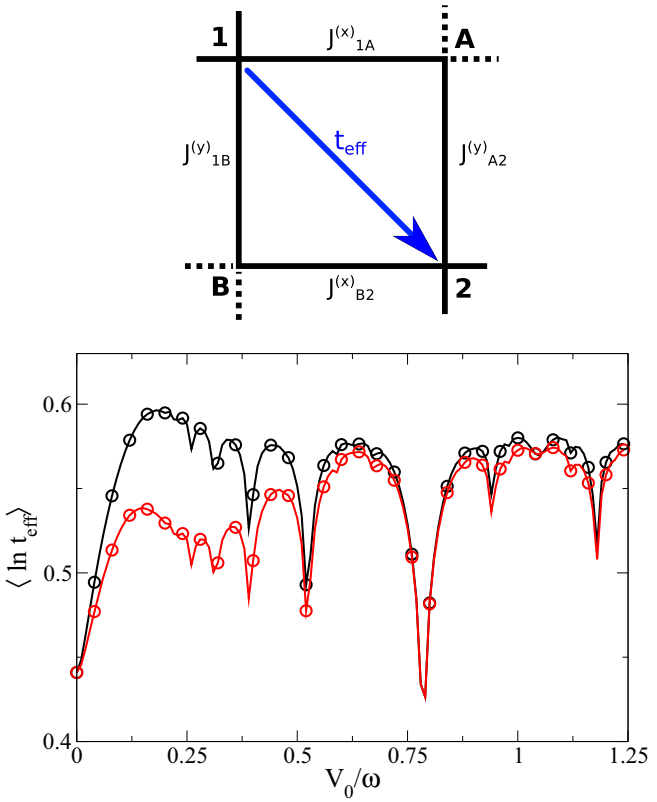

FIG. 3. Top panel: A single lattice plaquette. By cutting the outer connections at sites A and B, we could calculate tunneling through plaquette from site 1 to site 2 as given by (10). Bottom panel: The effective tunneling across the diagonal of the plaquette as a function of V_1/ω for uncorrelated (black circles) and correlated (red squares) of δ-type lattice modulations at a single energy E value. Similar behavior is observed at other energies.

MLL grows rapidly after the appearance of the random fluxes which is consistent with the growth of MLL expected when the time reversal symmetry is being broken. Surprisingly, for the correlated case, MLL grows much more slowly or even shows a small decrease.

In an attempt to understand this effect, we analyze the transport through a single plaquette disconnected from the lattice (as in Fig. 3, top panel). The effective tunneling through such a structure is calculated to be

$$t_{\text{eff}} = \frac{1}{E - V_0 n_A^{\text{f}}} J_{2A}^{(y)} J_{A1}^{(x)} + \frac{1}{E - V_0 n_B^{\text{f}}} J_{2B}^{(x)} J_{B1}^{(y)}, \qquad (10)$$

where the lattice sites are denoted as in Fig. 3 and E is energy of the state. We calculate t_{eff} for cases of the correlated and uncorrelated disorder (using the effective tunneling for the δ modulation case) and average it over disorder realizations. The results are shown in the lower panel of Fig. 3 versus the modulation parameter V_1/ω. As the states corresponding to MML have typically energies around $E = 3.15$, this energy is chosen for calculation of t_{eff} (the results qualitatively do not depend on E). We may observe qualitatatively similar behavior of t_{eff} for both correlated and uncorrelated disorder; for the latter the growth of t_{eff} is significantly faster. For

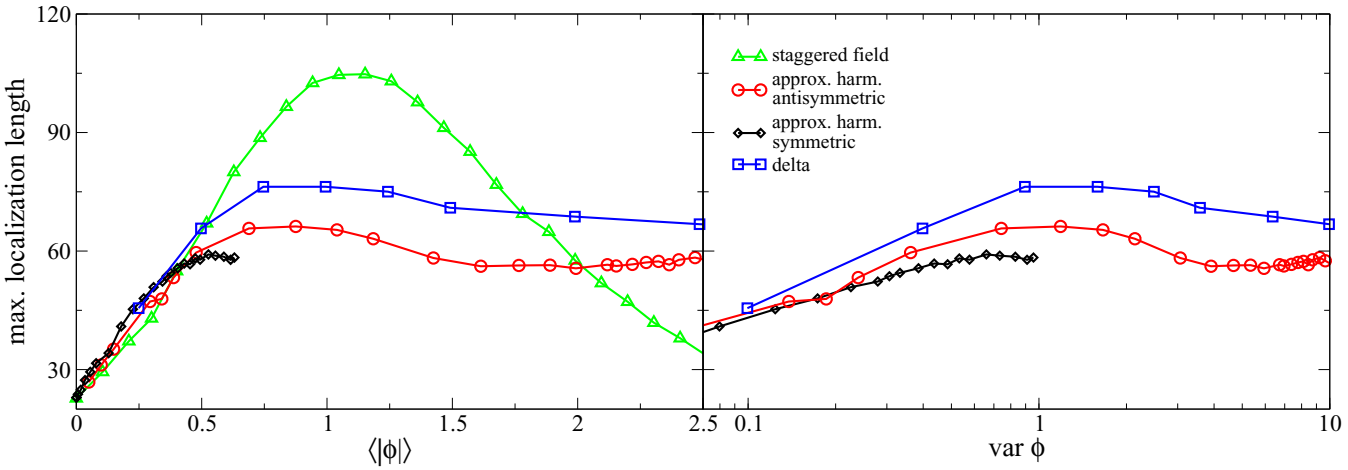

FIG. 4. Maximum localization length as a function of the mean of the absolute flux through a single plaquette (left) and as a function of the variance of the flux through plaquette (right). Results are presented for the case of no correlation between the diagonal and the off-diagonal disorder. Black diamonds correspond to the approximate symmetric harmonic modulation (8) while red circles to the approximate antisymmetric harmonic modulation ($t_1^{(x)} = -t_1^{(y)}$). Blue squares stand for the δ modulation (9) and green triangles denote for the pure diagonal disorder in the staggered field (lines are drawn to guide the eye).

sufficiently large $V_1/\omega > 0.7$ the difference between the two cases disappears.

Those results indicate that understanding of the surprising behavior observed for the correlated disorder cannot be obtained in the single plaquette model. Apparently the interference of different paths involving several plaquettes is responsible for the observed behavior for small and moderate V_1/ω.

As the correlations between the diagonal disorder and the flux disorder affect localization properties strongly, we should use results for the uncorrelated case to check the possible dependence of the MLL on the flux through a single plaquette. Plotting MLL for the uncorrelated case as a function of a mean absolute flux through lattice plaquette (Fig. 4, left panel), we can observe a similar behavior for the approximate harmonic modulation (for symmetric and antisymmetric versions) as well as for the δ modulation (we do not consider here the exact harmonic modulation as it gives also the disorder in absolute values of tunnelings, which obscures the effects discussed). For smaller V_1/ω values, those curves coincide with (also plotted) results for the diagonal disorder in the staggered field. This suggests that breaking of the time-reversal symmetry is a more important effect in this regime. For bigger fluxes, the results for the disordered systems start to diverge from one for the staggered field—this marks the region in which the random character of the fluxes gives a significant contribution to MLL. As we could see in the right panel of Fig. 4, all three models scale in similar manner also as a function of the variance of the flux.

For correlated disorder, the Anderson localization length can diverge for specific momenta. In the vicinity of such singularities, there are intervals of momenta values in which the localization length is typically very large, allowing atoms with those momenta to leave the finite system. In that way, the band-pass filter for momenta is formed, as wave functions for momenta outside of those (typically tiny) intervals remain Anderson localized. Such a mechanism has been proposed for BEC in speckle potential in one dimensional (1D) [47] and in periodically driven 1D optical lattice [34,48].

The model presented in this paper can be utilized to construct a band-pass filter for the center of energy band in two dimensions (2D). Using the example of studied above static disorder with amplitude $V_0 = 1.5$, let us consider an optical lattice system of size 30×30. All atoms are Anderson localized and remain in the system. Now, applying harmonic antisymmetric modulation with $V_1/\omega = 1$ MLL for $E \approx 4$ increases to 55 lattice site (Fig. 1) and atoms with energy distribution centered at $E \approx 4$ can escape from the system.

IV. CONCLUSIONS

In this paper, we have presented a method for creating two-dimensional disordered system with artificial random gauge field for the ultracold atoms in the optical lattice using fast periodic modulations of atoms interaction. We showed that the time-reversal symmetry breaking does not necessary lead to increase of the Anderson localization length. The presented model could be used to quantum simulation of high-T_c superconductors models where scattering on random gauge field could significantly lower the critical temperature [4].

ACKNOWLEDGMENTS

We are grateful to Dominique Delande for discussions. This research has been supported by the Polish National Science Center under Projects No. 2015/19/N/ST2/01677 (J.M.) and No. 2015/19/B/ST2/01028 (J.Z.). J.Z. acknowledges also support from PL-Grid Infrastructure and EU H2020-FETPROACT-2014 Project QUIC No. 641122. M.P. acknowledges support from the Foundation for Fundamental Research on Matter (FOM) and the Netherlands Organisation for Scientific Research (NWO).

[1] V. Kalmeyer and S.-C. Zhang, Phys. Rev. B **46**, 9889 (1992).
[2] B. I. Halperin, P. A. Lee, and N. Read, Phys. Rev. B **47**, 7312 (1993).
[3] J. K. Jain, Phys. Rev. Lett. **63**, 199 (1989).
[4] N. Nagaosa and P. A. Lee, Phys. Rev. Lett. **64**, 2450 (1990).
[5] F. Evers and A. D. Mirlin, Rev. Mod. Phys. **80**, 1355 (2008).
[6] D. Wiersma, P. Bartolini, and A. R. R. Lagendijk, Nature (London) **390**, 671 (1997).
[7] T. Schwartz, G. Bartal, S. Fishman, and M. Segev, Nature (London) **398**, 206 (1999).
[8] C. M. Aegerter, M. Störzer, S. Fiebig, W. Bührer, and G. Maret, Nature (London) **446**, 52 (2007).
[9] M. Segev, Y. Silberger, and D. N. Christodoulides, Nat. Photon. **7**, 197 (2013).
[10] P. Pradhan and S. Sridhar, Phys. Rev. Lett. **85**, 2360 (2000).
[11] H. Hu, A. Strybulevych, J. H. Page, S. E. Skipetrov, and B. A. van Tiggelen, Nat. Phys. **4**, 945 (2008).
[12] J. Billy, V. Josse, Z. Zuol, A. Bernard, B. Hambrecth, P. Lugan, D. Clement, L. Sanchez-Palecia, P. Bouyer, and A. Aspect, Nature (London) **453**, 891 (2008).
[13] G. Roati, C. D'Errico, L. Fallani, M. Fattori, C. Fort, M. Zaccanti, G. Modugno, M. Modugno, and I. Massimo, Nature (London) **453**, 895 (2008).
[14] S. S. Kondov, W. R. McGehee, J. J. Zirbel, and B. DeMarco, Science **334**, 66 (2011).
[15] B. Gadway, D. Pertot, J. Reeves, M. Vogt, and D. Schneble, Phys. Rev. Lett. **107**, 145306 (2011).
[16] F. Jendrzejewski, A. Bernard, K. Müller, P. Cheinet, V. Josse, M. Piraud, L. Pezzé, L. Sanchez-Palencia, A. Aspect, and P. Bouyer, Nat. Phys. **8**, 398 (2012).
[17] G. Semeghini, M. Landini, P. Castilho, S. Roy, G. Spagnolli, A. Trenkwalder, M. Fattori, M. Inguscio, and G. Modugno, Nat. Phys. **11**, 554 (2015).
[18] S. N. Evangelou and T. Ziman, J. Phys. C **20**, L235 (1987).
[19] C. Wang, Y. Su, Y. Avishai, Y. Meir, and X. R. Wang, arXiv:1411.4838.
[20] B. L. Altshuler, D. Khmel'nitzkii, A. I. Larkin, and P. A. Lee, Phys. Rev. B **22**, 5142 (1980).
[21] G. Bergmann, Phys. Rep. **107**, 1 (1984).
[22] N. Dupuis and G. Montambaux, Phys. Rev. Lett. **68**, 357 (1992).
[23] P. A. Lee and D. S. Fisher, Phys. Rev. Lett. **47**, 882 (1981).
[24] T. Sugiyama and N. Nagaosa, Phys. Rev. Lett. **70**, 1980 (1993).
[25] Y. Avishai, Y. Hatsugai, and M. Kohmoto, Phys. Rev. B **47**, 9561 (1993).
[26] D. Z. Liu, X. C. Xie, S. Das Sarma, and S. C. Zhang, Phys. Rev. B **52**, 5858 (1995).
[27] T. Kawarabayashi and T. Ohtsuki, Phys. Rev. B **51**, 10897 (1995).
[28] K. Yakubo and Y. Goto, Phys. Rev. B **54**, 13432 (1996).
[29] D. N. Sheng and Z. Y. Weng, Phys. Rev. Lett. **75**, 2388 (1995).
[30] X. C. Xie, X. R. Wang, and D. Z. Liu, Phys. Rev. Lett. **80**, 3563 (1998).
[31] A. Furusaki, Phys. Rev. Lett. **82**, 604 (1999).
[32] W. L. Chan, X. R. Wang, and X. C. Xie, Phys. Rev. B **54**, 11213 (1996).
[33] J. A. Vergés, Phys. Rev. B **57**, 870 (1998).
[34] A. Kosior, J. Major, M. Płodzień, and J. Zakrzewski, Phys. Rev. A **92**, 023606 (2015).
[35] O. Dutta, L. Tagliacozzo, M. Lewenstein, and J. Zakrzewski, Phys. Rev. A **95**, 053608 (2017).
[36] C. Chin, R. Grimm, P. Julienne, and E. Tiesinga, Rev. Mod. Phys. **82**, 1225 (2010).
[37] A. Rapp, X. Deng, and L. Santos, Phys. Rev. Lett. **109**, 203005 (2012).
[38] F. Meinert, M. J. Mark, K. Lauber, A. J. Daley, and H.-C. Nägerl, Phys. Rev. Lett. **116**, 205301 (2016).
[39] G. Floquet, Ann. Sci. Ec. Norm. Super. **12**, 47 (1883).
[40] M. Bukov, L. D'Alessio, and A. Polkovnikov, Adv. Phys. **64**, 139 (2015).
[41] A. Eckardt and E. Anisimovas, New J. Phys. **17**, 093039 (2015).
[42] T. Kuwahara, T. Mori, and K. Saito, Ann. Phys. **367**, 96 (2016).
[43] S. Blanes, F. Casas, J. Oteo, and J. Ros, Phys. Rep. **470**, 151 (2009).
[44] It is better than $O(1/\omega)$, which we will get if we have just proceeded with untransformed $H(t)$; however, in the rotating frame we will have $O(1/\omega^4)$.
[45] A. MacKinnon and B. Kramer, Z. Phys. B **53**, 1 (1983).
[46] E. Abrahams, P. W. Anderson, D. C. Licciardello, and T. V. Ramakrishnan, Phys. Rev. Lett. **42**, 673 (1979).
[47] M. Płodzień and K. Sacha, Phys. Rev. A **84**, 023624 (2011).
[48] J. Major, Phys. Rev. A **94**, 053613 (2016).